Commun. Theor. Phys. **68** (2017) 301–308 Vol. 68, No. 3, September 1, 2017

# A Novel Approach with Time-Splitting Spectral Technique for the Coupled Schrödinger–Boussinesq Equations Involving Riesz Fractional Derivative*

S. Saha Ray†

Department of Mathematics, National Institute Technology, Rourkela, Orissa-769008, India

(Received April 6, 2017; revised manuscript received May 22, 2017)

***Abstract*** *In the present paper the Riesz fractional coupled Schrödinger–Boussinesq (S-B) equations have been solved by the time-splitting Fourier spectral (TSFS) method. This proposed technique is utilized for discretizing the Schrödinger like equation and further, a pseudospectral discretization has been employed for the Boussinesq-like equation. Apart from that an implicit finite difference approach has also been proposed to compare the results with the solutions obtained from the time-splitting technique. Furthermore, the time-splitting method is proved to be unconditionally stable. The error norms along with the graphical solutions have also been presented here.*

**PACS numbers:** 02.30.Jr **DOI:** 10.1088/0253-6102/68/3/301
**Key words:** coupled Schrödinger–Boussinesq equations, Riesz fractional derivative, discrete fourier transform, inverse discrete Fourier transform

## 1 Introduction

The present paper deals with the following Riesz fractional coupled Schrödinger–Boussinesq equations

$$\begin{aligned} &\mathrm{i}\epsilon u_t - \frac{3}{2}(-\triangle)^{\alpha/2}u = \frac{1}{2}uv\,, \\ &x \in \Omega \subset \Re^+\,, \quad t > 0\,, \end{aligned} \tag{1}$$

$$\begin{aligned} &v_{tt} - v_{xx} - v_{xxxx} - (v^2)_{xx} = \frac{1}{4}(|u|^2)_{xx}\,, \\ &x \in \Omega \subset \Re^+\,, \quad t > 0\,, \end{aligned} \tag{2}$$

where the complex-valued function $u(x,t)$ represents the short wave amplitude and the real-valued function $v(x,t)$ represents the long wave amplitude and the parameter represents the mass ratio between the electron number and the ion number.

The field of fractional calculus is a vast and interesting area, which has not been fully explored yet. A large number of interesting and useful concepts have been emerging in the field of fractional calculus since its inception. The fractional order nonlinear partial differential equations (NPDEs) are used to describe and to have a good knowledge regarding many physical processes, like in signal processing, modelling anomalous dynamics of complex systems, control theory, fluid dynamics, viscoelasticity, rheology and biomechanics.[1–5] The Boussinesq-type equations are generally utilized in coastal engineering for the simulation of the water waves and shallow seas. Here our intention is to study the Schrödinger–Boussinesq equations by means of the time-splitting spectral method, which is a technique of finding the solution in small steps. It serves as a very powerful and effective technique for efficiently solving the nonlinear partial differential equations, as in Refs. [6–9]. In addition to this, in order to show the accuracy of the proposed technique, another method namely an implicit finite difference technique is employed to compare the solutions of both the techniques.

The literature regarding the numerical techniques and simulation of the Riesz fractional Schrödinger–Boussinesq (S-B) system is very much limited. So, some of the techniques presented here in the paper would prove to be highly desirable and effective. Bai and Wang[10] utilized the TSFS scheme to the Schrödinger–Boussinesq equations and performed numerical experiments for showing the numerical accuracy offered by the proposed method. Wang[11] utilized the time-splitting technique for the coupled Gross-Pitaevskii equations. Further, Markowich *et al.*[12] have applied the numerical approximation approach for the quadratic observables of Schrödinger-type equations in case of the semi-classical limit. Bai *et al.*[13] have studied the quadratic B-spline finite element method for the coupled S-B equations. Moreover, Liao *et al.*[14] have worked upon the compact finite difference technique for the coupled S-B equations. The same coupled equation is taken by Huang *et al.*[15] and performed the multi-sympletic scheme upon it. Furthermore, analysis of a linear conservative difference method for the coupled Schrödinger–Boussinesq equations is done by Liao *et al.*,[16] Zhang *et al.*[17] provided an analysis for a conservative scheme for the S-B equations.

This paper is set up in the following manner: firstly,

*Supported by NBHM, Mumbai, under Department of Atomic Energy, Government of India vide Grant No. 2/48(7)/2015/NBHM (R.P.)/R&D II/11403

†E-mail: santanusaharay@yahoo.com

some of the basic definitions regarding the Riesz fractional derivative have been exhibited in Sec. 2. Then, in Sec. 3, we describe the numerical techniques for the coupled S-B equations by presenting the Strang splitting scheme and subsequently the pseudospectral method for the given problem. Then stability analysis has been presented for the proposed scheme in Sec. 4. Moreover in Sec. 5, the spectral scheme is proved to be unconditionally stable. In Sec. 6, an implicit finite difference discretization is described for the proposed problem. Further in Sec. 7, the numerical experiments and discussions have been presented and along with that the tabulated results have been exhibited for the various solutions of $u(x,t)$ and $v(x,t)$. Furthermore, graphical solutions have been also exhibited here. Then Sec. 8 is devoted for the conclusion.

## 2 Mathematical Preliminaries of Fractional Calculus

### 2.1 *Riesz Derivative*

Here a definition regarding the Riesz fractional derivative has been provided with the aid of the Riemann–Liouville left and right fractional derivatives respectively.

***Definition 1*** The Riesz derivative of order $\alpha$ $(n-1<\alpha\leq n)$ on the infinite domain $-\infty<x<\infty$ is defined as[18]

$$\frac{\partial^\alpha f(x)}{\partial|x|^\alpha}=-c_\alpha\left({}_{-\infty}D_x^\alpha f(x)+{}_xD_\infty^\alpha f(x)\right), \tag{3}$$

where

$${}_{-\infty}D_x^\alpha f(x)=\frac{1}{\Gamma(n-\alpha)}\frac{\partial^n}{\partial x^n}\int_{-\infty}^x\frac{f(\xi)\mathrm{d}\xi}{(x-\xi)^{1-n+\alpha}}, \tag{4}$$

represents the Riemann–Liouville left fractional derivative and

$${}_xD_\infty^\alpha f(x)=\frac{(-1)^n}{\Gamma(n-\alpha)}\frac{\partial^n}{\partial x^n}\int_x^\infty\frac{f(\xi)\mathrm{d}\xi}{(\xi-x)^{1-n+\alpha}}, \tag{5}$$

represents the Riemann–Liouville right fractional derivative of order $\alpha$ $(n-1<\alpha\leq n)$ and

$$c_\alpha=\frac{1}{2\cos(\alpha\pi/2)},\quad \alpha\neq 1. \tag{6}$$

The Riesz derivative operator $(-\triangle)^{\alpha/2}$ is given by[2,19]

$$-(-\triangle)^{\alpha/2}f(x)=-\frac{\partial^\alpha f(x)}{\partial|x|^\alpha}, \tag{7}$$

for $n-1<\alpha\leq n$, $n\in\mathbb{N}$, $-\infty<x<\infty$.

***Remarks*** For a function $f(x)$ defined on the finite interval $[0,L]$, the above equality holds be setting

$$f^*(x)=\begin{cases}f(x), & x\in(0,L),\\ 0, & x\notin(0,L),\end{cases} \tag{8}$$

i.e. $f^*(x)=0$ on the boundary points and beyond the boundary points.

***Definition 2*** The Riesz–Feller fractional derivative of order $\alpha$, $0<\alpha\leq 2$, which is given as a pseudo-differential operator with the Fourier symbol $-|k|^\alpha$, $k\in\mathbb{R}$ is defined as in Refs. [2, 19]

$$\frac{\partial^\alpha f(x)}{\partial|x|^\alpha}=\mathcal{F}^{-1}[-|k|^\alpha\hat{f}(k)], \tag{9}$$

where

$$\mathcal{F}(f(x))=\hat{f}(k)=\int_{-\infty}^\infty \mathrm{e}^{\mathrm{i}kx}f(x)\mathrm{d}x. \tag{10}$$

## 3 Proposed Technique for Riesz Fractional Coupled Schrödinger–Boussinesq Equations

In the present analysis, an efficient numerical technique has been used for solving the following Schrödinger–Boussinesq equations with Riesz fractional derivative

$$\mathrm{i}\epsilon u_t-\frac{3}{2}(-\triangle)^{\alpha/2}u=\frac{1}{2}uv,\quad a<x<b,\quad t>0, \tag{11}$$

$$v_{tt}-v_{xx}-v_{xxxx}-(v^2)_{xx}=\frac{1}{4}(|u|^2)_{xx},$$
$$a<x<b,\quad t>0, \tag{12}$$

with initial conditions

$$u(x,0)=\gamma_0(x),\quad v(x,0)=\eta_0(x),$$
$$v_t(x,0)=\eta_1(x),\quad a\leq x\leq b. \tag{13}$$

Here the discretization is done in the following way. The mesh size is taken as $h=(b-a)/m$ where $m$ is an even integer. The grid points are taken as $x_j=a+jh$, $j=0,1,\ldots,m$ and the time steps be taken as $t_n=n\tau$, $\tau>0$, $n=0,1,\ldots$ The Schrödinger-like Eq. (11) is solved in two splitting steps from $t_n$ to $t_{n+1}$ for the time step $\tau$,

$$\mathrm{i}\epsilon u_t-\frac{3}{2}(-\triangle)^{\alpha/2}=0, \tag{14}$$

and subsequently solving

$$\mathrm{i}\epsilon u_t=\frac{1}{2}uv, \tag{15}$$

by taking the same time step.

Firstly, by using the Fourier spectral method Eq. (14) will be discretized in space and then integrating Eq. (15) in time from $t_n$ to $t_{n+1}$, and consequently utilizing the trapezoidal rule to approximate the integral on $[t_n,t_{n+1}]$, we obtain

$$u(x,t_{n+1})=\exp\Big[\int_{t_n}^{t_{n+1}}\Big(-\frac{\mathrm{i}}{2\epsilon}v(x,s)\Big)\mathrm{d}s\Big]u(x,t_n)$$
$$=\exp\Big[-\frac{\mathrm{i}}{4\epsilon}\tau(v(x,t_n)+v(x,t_{n+1}))\Big]u(x,t_n). \tag{16}$$

From Eq. (14), we have

$$u_t=-\frac{3\mathrm{i}}{2\epsilon}(-\triangle)^{\alpha/2}u. \tag{17}$$

Now applying Fourier transform, and then integrating Eq. (17), we obtain

$$\hat{u}(\mu_k,t_{n+1})=\exp\Big(-\frac{3\mathrm{i}}{2\epsilon}|\mu_k|^\alpha\tau\Big)\hat{u}(\mu_k,t_n), \tag{18}$$

where $\mu_k$ is taken as

$$\mu_k = \frac{2\pi k}{b-a}\,. \tag{19}$$

Now the discrete Fourier transformation from $t = t_n$ to $t_{n+1}$ of the sequence $(\phi_j)$ is defined as

$$\hat{\phi}_k(t) = F_k[\phi_j(t)] = \sum_{j=0}^{m-1} \phi_j(t)\exp(-\mathrm{i}\mu_k x_j)\,,$$
$$k = -\frac{m}{2},\ldots,\frac{m}{2}-1\,. \tag{20}$$

Consequently, the inverse discrete Fourier transform for Eq. (20) is given by

$$\phi_j(t) = F_j^{-1}[\hat{\phi}_k(t)] = \frac{1}{m}\sum_{k=-m/2}^{m/2-1} \hat{\phi}_k(t)\exp(\mathrm{i}\mu_k x_j)\,,$$
$$j = 0,1,\ldots,m-1\,. \tag{21}$$

Now, the inverse discrete Fourier transform to Eq. (18) yields

$$u_j^{**} = \frac{1}{m}\sum_{k=-m/2}^{m/2-1} \exp\Big(-\frac{3\mathrm{i}}{2\epsilon}|\mu_k|^{\alpha}\tau\Big)(\hat{u}^*)_k\exp(\mathrm{i}\mu_k x_j)\,, \tag{22}$$

where

$$(\hat{u}^*)_k = \sum_{j=0}^{m-1} u_j^*\exp(\mathrm{i}\mu_k x_j)\,,\quad k = -\frac{m}{2},\ldots,\frac{m}{2}-1\,. \tag{23}$$

### 3.1 *Second Order Splitting Scheme or Strang Splitting (SP) Scheme*

The Strang splitting scheme for the Schrödinger-like Eq. (11) is shown as

$$u_j^* = \exp\Big[-\frac{i\tau}{4\epsilon}(v_j^{n+1}+v_j^n)\Big]u_j^n\,,$$
$$j = 0,1,\ldots,m-1\,, \tag{24}$$

$$u_j^{**} = \frac{1}{m}\sum_{k=-m/2}^{m/2-1} \exp\Big(-\frac{3\mathrm{i}}{2\epsilon}|\mu_k|^{\alpha}\tau\Big)(\hat{u}^*)_k\exp(\mathrm{i}\mu_k x_j)\,,$$
$$j = 0,1,\ldots,m-1\,, \tag{25}$$

$$u_j^{n+1} = \exp\Big[-\frac{\mathrm{i}\tau}{4\epsilon}(v_j^{n+1}+v_j^n)\Big]u_j^{**}\,,$$
$$j = 0,1,\ldots,m-1\,, \tag{26}$$

where

$$(\hat{u}^*)_k = \sum_{j=0}^{m-1} u_j^*\exp(-\mathrm{i}\mu_k x_j)\,,\quad k = -\frac{m}{2},\ldots,\frac{m}{2}-1 \tag{27}$$

are the Fourier coefficients of $u^*$.

### 3.2 *Pseudospectral Scheme*

For Eq. (12), the spatial derivatives are approximated via the pseudospectral method. Here we make use of a spectral differential operator approximating $\partial_{xx}$, is defined as

$$D_{xx}U|_{x=x_j} = \frac{1}{m}\sum_{k=-m/2}^{m/2-1}(i\mu_k)^2\hat{U}_j\exp(\mathrm{i}\mu_k x_j)$$
$$= \mathcal{F}^{-1}((\mathrm{i}\mu_k)^2\hat{U}_j)\,, \tag{28}$$

and similarly defining

$$D_{xxxx}U|_{x=x_j} = \frac{1}{m}\sum_{k=-m/2}^{m/2-1}(\mathrm{i}\mu_k)^4\hat{U}_j\exp(\mathrm{i}\mu_k x_j)\,, \tag{29}$$

for approximating the fourth order partial derivative. Here $\hat{U}_j$ is defined as

$$\hat{U}_j = \sum_{j=0}^{m-1} U_j\exp(-\mathrm{i}\mu_k x_j)\,,$$
$$k = -\frac{m}{2},\ldots,\frac{m}{2}-1\,. \tag{30}$$

Now utilizing the implicit finite difference scheme due to Crank–Nicolson leap frog spectral method, we obtain

$$v_j^{n+1} - 2v_j^n + v_j^{n-1}/\tau^2$$
$$- D_{xx}(\theta v^{n+1} + (1-2\theta)v^n + \theta v^{n-1})|_{x=x_j}$$
$$- D_{xxxx}(\theta v^{n+1} + (1-2\theta)v^n + \theta v^{n-1})|_{x=x_j}$$
$$- D_{xx}(\theta(v^{n+1})^2 + (1-2\theta)(v^n)^2$$
$$+ \theta(v^{n-1})^2)|_{x=x_j} = \frac{1}{4}D_{xx}(|u_j^n|^2)\,, \tag{31}$$

where $0 \le \theta \le 1/2$ is a constant.

Now putting

$$v_j^n = \frac{1}{m}\sum_{k=-m/2}^{m/2-1}(\hat{v}^n)_k\exp(\mathrm{i}\mu_k x_j) \tag{32}$$

into Eq. (31) and using the definition in Eqs. (28) and (29), we obtain

$$(\hat{v}^{n+1})_k - 2(\hat{v}^n)_k + (\hat{v}^{n-1})_k/\tau^2$$
$$- (\mathrm{i}\mu_k)^2[\theta(\hat{v}^{n+1})_k + (1-2\theta)(\hat{v}^n)_k + \theta(\hat{v}^{n-1})_k]$$
$$- (\mathrm{i}\mu_k)^4[\theta(\hat{v}^{n+1})_k + (1-2\theta)(\hat{v}^n)_k + \theta(\hat{v}^{n-1})_k]$$
$$- (\mathrm{i}\mu_k)^2[\theta((\hat{v}^{n+1})_k)^2 + (1-2\theta)((\hat{v}^n)_k)^2$$
$$+ \theta((\hat{v}^{n-1})_k)^2] = \frac{(\mathrm{i}\mu_k)^2}{4}\mathcal{F}^{-1}(F_k(|u^n|^2))\,,$$

for $t_n \le t \le t_{n+1}$.

***Note*** The spectral accuracy of the time-splitting spectral method is of spectral order accuracy in $h$ and second order accuracy in $\tau$.

## 4 Properties and Stability Analysis

Let us define $L^2$-norm and discrete $l^2$-norm as

$$||\boldsymbol{u}||_{L^2} = \sqrt{\int_a^b |u(x)|^2\,\mathrm{d}x}\,,$$

$$||\boldsymbol{u}||_{l^2} = \sqrt{\frac{b-a}{m}\sum_{j=0}^{m-1}|u_j|^2}\,. \tag{33}$$

***Theorem 1***

The time-splitting scheme (24), (25), and (26) for the Schrödinger–Boussinesq equations is unconditionally stable and possess the following conservative properties:

$$||\boldsymbol{u}^{n+1}||_{l^2}^2 = ||u^0||_{l^2}^2\,, \quad n = 0, 1, 2, \ldots \tag{34}$$

***Proof*** For the scheme (24)–(26), using Eqs. (21), (22), and (33), we have

$$\begin{aligned}
\frac{1}{b-a}||\boldsymbol{u}^{n+1}||_{l^2}^2 &= \frac{1}{m}\sum_{j=0}^{m-1}|u_j^{n+1}|^2 = \frac{1}{m}\sum_{j=0}^{m-1}\Big|\exp\Big(-\frac{\mathrm{i}\tau}{4\epsilon}(v_j^{n+1}+v_j^n)\Big)u_j^{**}\Big|^2 = \frac{1}{m}\sum_{j=0}^{m-1}|u_j^{**}|^2\\
&= \frac{1}{m}\sum_{j=0}^{m-1}\Big|\frac{1}{m}\sum_{k=-m/2}^{m/2-1}\exp\Big(-\frac{3\mathrm{i}}{2\epsilon}|\mu_k|^\alpha\tau\Big)(\hat{u}^*)_k\exp(\mathrm{i}\mu_k x_j)\Big|^2 = \frac{1}{m^2}\sum_{k=-m/2}^{m/2-1}\Big|\exp\Big(-\frac{3\mathrm{i}}{2\epsilon}|\mu_k|^\alpha\tau\Big)(\hat{u}^*)_k\Big|^2\\
&= \frac{1}{m^2}\sum_{k=-m/2}^{m/2-1}|(\hat{u}^*)_k|^2 = \frac{1}{m^2}\sum_{k=-m/2}^{m/2-1}\Big|\sum_{j=0}^{m-1}u_j^*\exp(-\mathrm{i}\mu_k x_j)\Big|^2 = \frac{1}{m}\sum_{j=0}^{m-1}|u_j^*|^2\\
&= \frac{1}{m}\sum_{j=0}^{m-1}\Big|\exp\Big(-\frac{\mathrm{i}\tau}{4\epsilon}(v_j^{n+1}+v_j^n)\Big)u_j^n\Big|^2 = \frac{1}{m}\sum_{j=0}^{m-1}|u_j^n|^2 = \frac{1}{b-a}||\boldsymbol{u}^n||_{l_2}^2\,.
\end{aligned} \tag{35}$$

The stability of the time-splitting spectral approximation for the fractional coupled Schrödinger–Boussinesq equations manifests that the total density is conserved in the discretized level.

## 5 Von Neumann Stability Analysis for Proposed Spectral Scheme

***Theorem 2*** The scheme in Eq. (31) is unconditionally stable for $1/4 \le \theta \le 1/2$ and for $0 \le \theta < 1/4$, the scheme is conditionally stable with condition

$$\tau \le \min_{-m/2\le k\le m/2-1, k\ne 0}\sqrt{4/(4\theta-1)(16\pi^4k^4 - 4\pi^2k^2(b-a)^2(1+B)/(b-a)^4)}\,. \tag{36}$$

***Proof*** Let $\xi$ be the amplification factor. First of all plugging $(\hat{v}^{n+1})_k = \xi(\hat{v}^n)_k = \xi^2(\hat{v}^{n-1})_k$ and $(\hat{\phi}^{n+1})_k = \xi(\hat{\phi}^n)_k = \xi^2(\hat{\phi}^{n-1})_k$, where $\phi = v^2$ into the discretization scheme (31), we get

$$\begin{aligned}
&\frac{\xi^2(\hat{v}^{n-1})_k - 2\xi(\hat{v}^{n-1})_k + (\hat{v}^{n-1})_k}{\tau^2} + (\mu_k)^2(\theta\xi^2(\hat{v}^{n-1})_k + (1-2\theta)\xi(\hat{v}^{n-1})_k + \theta(\hat{v}^{n-1})_k) - (\mu_k)^4(\theta\xi^2(\hat{v}^{n-1})_k\\
&\quad + (1-2\theta)\xi(\hat{v}^{n-1})_k + \theta(\hat{v}^{n-1})_k) + (\mu_k)^2(\theta\xi^2(\hat{\phi}^{n-1})_k + (1-2\theta)\xi(\hat{\phi}^{n-1})_k + \theta(\hat{\phi}^{n-1})_k) = 0\,,
\end{aligned}$$

which gives the characteristic equation

$$\xi^2 + \Big[\frac{-2-\tau^2(1-2\theta)(\mu_k^4 - \mu_k^2 - \mu_k^2B)}{1-\tau^2\theta(\mu_k^4-\mu_k^2-\mu_k^2B)}\Big]\xi + 1 = 0\,, \tag{37}$$

where $B = (\hat{\phi}^{n-1})_k/(\hat{v}^{n-1})_k$.

Let $\mu_k^4 - \mu_k^2 - \mu_k^2B = w$.

According to Lemma 1 of Ref. [10] the root of the Eq. (37) satisfies $|\xi| \le 1$ if and only if

$$\Big|\frac{2+\tau^2w(1-2\theta)}{1-\tau^2\theta w}\Big| \le 2\,. \tag{38}$$

So when $1/4 < \theta \le 1/2$, we obtain

$$-1 \le \tau^2 w\Big(\frac{1}{4}-\theta\Big)\,. \tag{39}$$

So Eq. (38) is hold for any value of $\tau$. Hence, the proposed scheme is unconditionally stable for $1/4 < \theta \le 1/2$.

Now when $0 \le \theta < 1/4$, we obtain

$$\tau^2 \le \frac{-1}{(1/4-\theta)w}\,. \tag{40}$$

So for the case $0 \le \theta < 1/4$, the stability condition is given by

$$\tau \le \sqrt{\frac{4}{(4\theta-1)w}}\,, \tag{41}$$

by which we obtain the following stability condition

$$\tau \le \min_{-m/2\le k\le m/2-1, k\ne 0}\sqrt{\frac{4}{(4\theta-1)(\mu_k^4-\mu_k^2-\mu_k^2B)}}\,. \tag{42}$$

Hence,

$$\tau \le \min_{-m/2\le k\le m/2-1, k\ne 0}\sqrt{\frac{4}{(4\theta-1)\{[16\pi^4k^4 - 4\pi^2k^2(b-a)^2(1+B)]/(b-a)^4\}}}\,, \tag{43}$$

since $\mu_k = 2\pi k/(b-a)$. ■

## 6 Implicit Finite Difference Scheme with Fractional Centered Difference

The approximation of Riesz fractional derivative by fractional centered difference is done in the following way. It can be shown that[20]

$$\lim_{h\to 0}\frac{\triangle_h^\alpha\theta(x)}{h^\alpha}=\lim_{h\to 0}\frac{1}{h^\alpha}\sum_{j=-\infty}^{\infty}\frac{(-1)^j\Gamma(\alpha+1)}{\Gamma(\alpha/2-j+1)\Gamma(\alpha/2+j+1)}\theta(x-jh)\,, \tag{44}$$

represents the Riesz fractional derivative Eq. (3) for the case of $1<\alpha\leq 2$.

***Lemma 1*** Let $f\in C^5(\mathbb{R})$ with all the derivatives up to fifth order belong to the space $L_1(\mathbb{R})$ and

$$\triangle_h^\alpha f(x)=\sum_{j=-\infty}^{\infty}\frac{(-1)^j\Gamma(\alpha+1)}{\Gamma(\alpha/2-j+1)\Gamma(\alpha/2+j+1)}f(x-jh)\,. \tag{45}$$

be the fractional centered difference, then

$$-h^{-\alpha}\,\triangle_h^\alpha\, f(x)=\frac{\partial^\alpha f(x)}{\partial|x|^\alpha}+O(h^2)\,. \tag{46}$$

So here when $h\to 0$, $\partial^\alpha f(x)/\partial|x|^\alpha$ represents the Riesz derivative of fractional order $\alpha$ for $1<\alpha\leq 2$.

***Proof*** It may be referred to Ref. [20] for the proof of above result.

***Corollary*** In the recent work (see Ref. [20]), it can be shown that if $f^*(x)$ is defined by

$$f^*(x)=\begin{cases} f(x)\,, & x\in[a,b]\,,\\ 0\,, & x\notin[a,b]\,,\end{cases} \tag{47}$$

such that $f^*\in C^5(\mathbb{R})$ and all derivatives upto order five belongs to the space $L_1$ $(\mathbb{R})$, then for the Riesz derivative of fractional order $\alpha$ $(1<\alpha\leq 2)$

$$\frac{\partial^\alpha f(x)}{\partial|x|^\alpha}=-h^{-\alpha}\sum_{j=-(b-x)/h}^{(x-a)/h}\frac{(-1)^j\Gamma(\alpha+1)}{\Gamma(\alpha/2-j+1)\Gamma(\alpha/2+j+1)}f(x-jh)+O(h^2)\,, \tag{48}$$

where $h=(b-a)/m$ and $m$ denotes the number of subintervals of the interval $[a,b]$.

### 6.1 *Implicit Finite Difference Scheme for Riesz Fractional Coupled Schrödinger–Boussinesq Equations*

Now the second-order implicit finite difference discretization for Eq. (11) is

$$\mathrm{i}\epsilon\Big(\frac{u_i^{n+1}-u_i^n}{\tau}\Big)+\frac{3}{4}(-h^{-\alpha})\Big(\sum_{j=i-m}^{i}g_j u_{i-j}^{n+1}+\sum_{j=i-m}^{i}g_j u_{i-j}^{n}\Big)=\frac{1}{4}\Big(v_i^{n+1}u_i^{n+1}+v_i^n u_i^n\Big)+R_i^{n+1/2}\,, \tag{49}$$

where the local truncation error $R_i^{n+1/2}=O(\tau^2+h^2)$. The second-order implicit finite difference discretization for Eq. (12) is

$$\begin{aligned}&\frac{v_j^{n+1}-2v_j^n+v_j^{n-1}}{\tau^2}-\frac{1}{4}\Big(\frac{v_{j+1}^{n-1}-2v_j^{n-1}+v_{j-1}^{n-1}}{h^2}+2\Big(\frac{v_{j+1}^{n}-2v_j^{n}+v_{j-1}^{n}}{h^2}\Big)+\frac{v_{j+1}^{n+1}-2v_j^{n+1}+v_{j-1}^{n+1}}{h^2}\Big)\\
&\quad-\frac{1}{4}\Big(\frac{v_{j+2}^{n-1}-4v_{j+1}^{n-1}+6v_j^{n-1}-4v_{j-1}^{n-1}+v_{j-2}^{n-1}}{h^4}+2\Big(\frac{v_{j+2}^{n}-4v_{j+1}^{n}+6v_j^{n}-4v_{j-1}^{n}+v_{j-2}^{n}}{h^4}\Big)\Big)\\
&\quad-\frac{1}{4}\Big(\frac{v_{j+2}^{n+1}-4v_{j+1}^{n+1}+6v_j^{n+1}-4v_{j-1}^{n+1}+v_{j-2}^{n+1}}{h^4}\Big)-\frac{1}{4}\Big(\frac{\phi_{j+1}^{n-1}-2\phi_j^{n-1}+\phi_{j-1}^{n-1}}{h^2}+2\Big(\frac{\phi_{j+1}^{n}-2\phi_j^{n}+\phi_{j-1}^{n}}{h^2}\Big)\Big)\\
&\quad-\frac{1}{4}\Big(\frac{\phi_{j+1}^{n+1}-2\phi_j^{n+1}+\phi_{j-1}^{n+1}}{h^2}\Big)\\
&=\frac{1}{16}\Big(\frac{\psi_{j+1}^{n-1}-2\psi_j^{n-1}+\psi_{j-1}^{n-1}}{h^2}+2\Big(\frac{\psi_{j+1}^{n}-2\psi_j^{n}+\psi_{j-1}^{n}}{h^2}\Big)+\frac{\psi_{j+1}^{n+1}-2\psi_j^{n+1}+\psi_{j-1}^{n+1}}{h^2}\Big)+R_i^n\,,\end{aligned}$$

where $\psi=|u|^2$ and the local truncation error $R_i^n=O(\tau^2+h^2)$.

## 7 Numerical Experiments and Discussions

***Example 1*** We consider the S-B Eqs. (11) and (12) with the given initial conditions[10]

$$\begin{aligned}\gamma_0(x)&=8\sqrt{3}\lambda\,\mathrm{sech}\,(\rho x)\tanh(\rho x)\,\mathrm{e}^{\,\mathrm{i}kx}\,,\\ \eta_0(x)&=-6\lambda\,\mathrm{sech}^{\,2}(\rho x)\,,\\ \eta_1(x)&=-12\rho\lambda m\,\mathrm{sech}^{\,2}(\rho x)\tanh(\rho x)\,,\end{aligned}$$

where $\rho=\sqrt{3}/15$, $\lambda=0.04$ and $k=\sqrt{165}/45$ for the

fractional coupled S-B equations. In this case, we take the spatial interval as $[-20\pi, 20\pi]$ and the mass ratio $\epsilon = 1$.

***Example 2*** We consider the S-B Eqs. (11) and (12) with the given initial conditions[10]

$$\gamma_0(x) = 2\,\mathrm{e}^{\mathrm{i}x}\,, \quad \eta_0(x) = 1\,, \quad \eta_1(x) = 0\,,$$

with the spatial interval $[a, b]$ as $[0, 4\pi]$ and $\epsilon = 1$.

In the following numerical discussion, the error norms for the solutions in Example 1 have been calculated and shown in Table 1. These error norms are calculated with regard to implicit finite difference results and time-splitting spectral approximations. Next, when $t = 1.0$, the absolute errors for coupled Schrödinger–Boussinesq equations (11) and (12) obtained by using time-splitting Fourier spectral approximation and the implicit(IFDM) finite difference approach at various points of $x$ have been presented in Table 2, taking step size $\tau = 0.1$ and $\alpha = 1.5$.

In the present analysis, the error norms $L_2$ and $L_\infty$ are presented in Table 1. Here, in this case, for a fixed time $t_l$, the $L_2$ norm for error is given by

$$L_2 \equiv \sqrt{\frac{1}{2m+1}\sum_{i=1}^{2m+1}(u_{\mathrm{TSFS}}(x_i, t_l) - u_{\mathrm{IFDM}}(x_i, t_l))^2}\,,$$

and the $L_\infty$ norm for error is given by

$$L_\infty \equiv \max_{-m\le i\le m} |u_{\mathrm{TSFS}}(x_i, t_l) - u_{\mathrm{IFDM}}(x_i, t_l)|\,.$$

**Table 1** $L_2$ norm and $L_\infty$ norm of errors between the solutions of TSFS method and implicit finite difference method for Example 1 at $t = 1$, when $\alpha = 1.5$.

| $t$ | $\alpha = 1.5$<br>$L_2$ error of $\lvert u(x,t)\rvert$ | $\alpha = 1.5$<br>$L_\infty$ error of $\lvert u(x,t)\rvert$ | $\alpha = 1.5$<br>$L_2$ error of $v(x,t)$ | $\alpha = 1.5$<br>$L_\infty$ error of $v(x,t)$ |
|---|---|---|---|---|
| 1.0 | $3.69404\times10^{-4}$ | $1.76402\times10^{-3}$ | $1.25959\times10^{-5}$ | $4.22961\times10^{-5}$ |

**Table 2** Absolute errors for coupled Schrödinger–Boussinesq equations (11) and (12) obtained by using time-splitting Fourier spectral approximation and the implicit finite difference solutions for Example 1 at various points of $x$ and $t = 1.0$ taking step size $\tau = 0.1$ and $\alpha = 1.5$.

| $x$ | $t = 1.0$ ($\alpha = 1.5$)<br>Absolute error between<br>$\lvert u\rvert_{\mathrm{TSFS}}$ and $\lvert u\rvert_{\mathrm{IFDM}}$ | $t = 1.0$ ($\alpha = 1.5$)<br>Absolute error between<br>$v_{\mathrm{TSFS}}$ and $v_{\mathrm{IFDM}}$ |
|---|---|---|
| –62.8319 | $5.251\,31\times10^{-4}$ | $4.229\,61\times10^{-5}$ |
| –58.9049 | $5.953\,31\times10^{-5}$ | $2.942\,38\times10^{-5}$ |
| –52.0326 | $2.290\,29\times10^{-5}$ | $1.196\,75\times10^{-5}$ |
| –46.1421 | $1.301\,17\times10^{-6}$ | $6.671\,05\times10^{-6}$ |
| –38.2882 | $4.972\,08\times10^{-6}$ | $3.575\,22\times10^{-6}$ |
| –30.4342 | $6.138\,57\times10^{-5}$ | $2.334\,15\times10^{-6}$ |
| –22.5802 | $9.748\,55\times10^{-5}$ | $1.796\,47\times10^{-6}$ |
| –12.7627 | $4.633\,32\times10^{-4}$ | $1.2169\times10^{-6}$ |
| –0.981 74 | $1.764\,02\times10^{-3}$ | $6.868\,71\times10^{-6}$ |
| 0.981 74 | $1.301\,42\times10^{-3}$ | $1.387\,43\times10^{-5}$ |
| 12.7627 | $5.347\,11\times10^{-5}$ | $4.085\,33\times10^{-6}$ |
| 22.5802 | $1.237\,68\times10^{-4}$ | $1.2136\times10^{-6}$ |
| 30.4342 | $5.0682\times10^{-5}$ | $2.609\,35\times10^{-6}$ |

Apart from the above tabulated results, the graphical solutions have been plotted separately for $|u(x,t)|$ and $v(x,t)$ at various points of $x$ and $t = 1.0$. In Fig. 1(a), the solutions for the absolute values of complex-valued function $u(x,t)$ obtained by the time-splitting Fourier spectral (TSFS) method for Example 1 have been plotted for the spatial interval $-20\pi \le x \le 20\pi$ and at $t = 1.0$ by taking fractional order $\alpha = 1.5$. Similarly, in Fig. 1(b), the TSFS solutions for $v(x,t)$ for Example 1 have been plotted for the same interval $-20\pi \le x \le 20\pi$ and $t = 1.0$ taking $\alpha = 1.5$. In Fig. 2(a), comparison of graphs have been shown for the solutions of $|u(x,t)|$ obtained from TSFS method and implicit finite difference scheme for coupled Schrödinger–Boussinesq equations (11) and (12) for Example 1 at $t = 1.0$. Similarly Fig. 2(b) manifests the comparison of graphs for the solutions of $v(x,t)$ obtained from TSFS method and implicit finite difference scheme for coupled Schrödinger–Boussinesq equations (11) and (12) for Example 1 at $t = 1.0$ and $\alpha = 1.5$. In Fig. 3, the solutions for the real values of complex-valued func-

tion $u(x,t)$ obtained by the time-splitting Fourier spectral (TSFS) method for Example 2 have been plotted for the spatial interval $0 \leq x \leq 4\pi$ and at $t = 1.0$ by taking fractional order $\alpha = 1.5$. Similarly, in Fig. 4, the TSFS solutions for $\mathrm{Im}\,(u(x,t))$ for Example 2 has been plotted for the same interval $0 \leq x \leq 4\pi$ and $t = 1.0$ taking $\alpha = 1.5$.

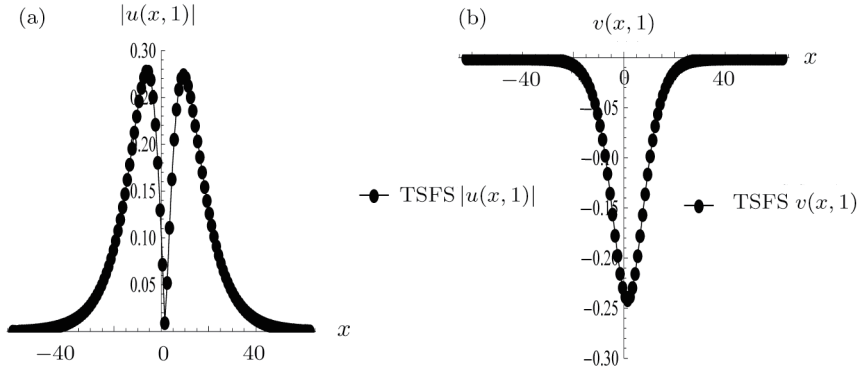


**Fig. 1** (a) Two Soliton wave 2-D solutions of $|u(x,t)|$ of Example 1 for the Riesz fractional coupled Schrödinger–Boussinesq equations for various points of $x$ at $t = 1.0$ for $\alpha = 1.5$ and (b) One Soliton wave 2-D solution of $v(x,t)$ of Example 1 for the Riesz fractional coupled Schrödinger–Boussinesq equations for various points of $x$ at $t = 1.0$ for $\alpha = 1.5$.

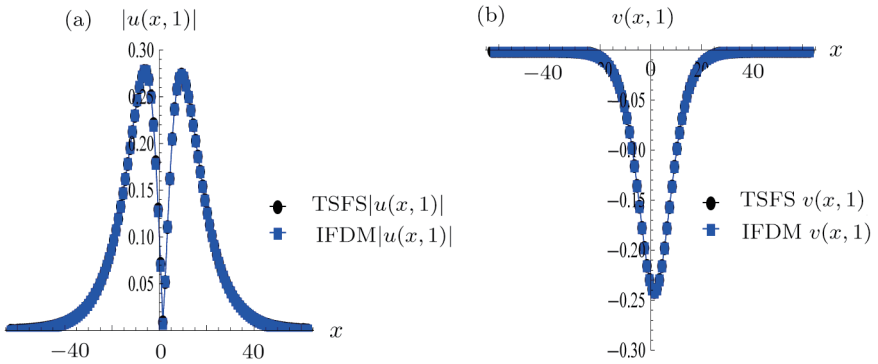


**Fig. 2** (a) Comparison of graphs for the solutions of $|u(x,t)|$ obtained from TSFS method and implicit finite difference scheme for the Riesz fractional coupled Schrödinger–Boussinesq equations (11) and (12) for Example 1 at $t = 1.0$ and (b) Comparison of graphs for the solutions of $v(x,t)$ obtained from TSFS method and implicit finite difference scheme for the Riesz fractional coupled Schrödinger–Boussinesq equations (11) and (12) for Example 1 at $t = 1.0$.

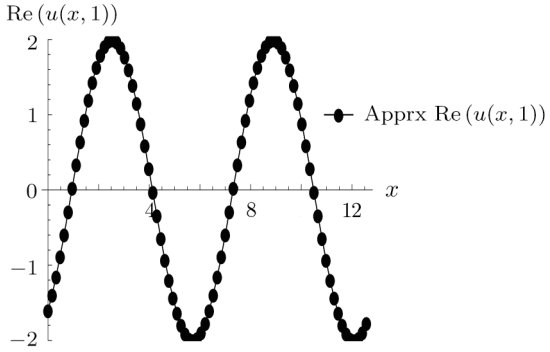


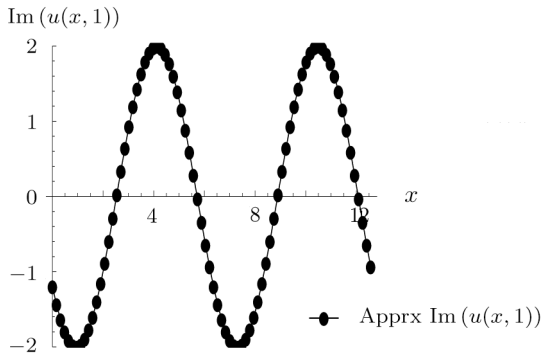


**Fig. 3** Periodic wave 2-D solution of $\mathrm{Re}\,(u(x,t))$ of Example 2 for the Riesz fractional coupled Schrödinger–Boussinesq equations by TSFS method for various points of $x$ at for $t = 1.0$ and $\alpha = 1.5$.

**Fig. 4** Periodic wave 2-D solution of $\mathrm{Im}\,(u(x,t))$ of Example 2 for the Riesz fractional coupled Schrödinger–Boussinesq equations by TSFS method for various points of $x$ at for $t = 1.0$ and $\alpha = 1.5$.

## 8 Conclusion

The time-splitting Fourier spectral technique has been utilized here for the Riesz fractional coupled Schrödinger–Boussinesq (S-B) Eqs. (11) and (12). The time splitting spectral scheme is found to be unconditionally stable. Furthermore, the employed method is found to be very satisfactory and efficient. In addition, an implicit finite difference method is used for solving the S-B equations and the results obtained by this method have been compared with the solutions of TSFS method and there is a good agreement between the solutions of both the methods. Moreover in order to exhibit the accuracy of the proposed method, the results have been graphically presented. The graphs of Example 1 exhibit the two soliton 2-D solutions of $|u(x,1)|$ and one soliton 2-D solution of $v(x,1)$ respectively. On the other hand, the graphs of Example 2 manifest the periodic nature of wave solutions.

## Acknowledgments

The authors take the prerogative through this opportunity to express their heartfelt thanks and gratitude to the anonymous learned reviewer for his valuable comments and suggestions for the improvement and betterment of the manuscript. The review comments and suggestions of the learned reviewer are highly apprciable and praiseworthy.

# References

[1] I. Podlubny, *Fractional Differential Equations*, Academic press, New York (1999).

[2] S. G. Samko, A. A. Kilbas, and O. I. Marichev, *Fractional Integrals and Derivatives: Theory and Applications*, Springer, New York (1993).

[3] S. Saha Ray, *Fractional Calculus with Applications for Nuclear Reactor Dynamics*, CRC Press, Taylor and Francis group, Boca Raton, New York (2016).

[4] K. B. Oldham and J. Spanier, *The Fractional Calculus*, Academic Press, New York, USA (1974).

[5] K. S. Miller and B. Ross, *An Introduction to Fractional Calculus and Fractional Differential Equations*, John Wiley, New York, USA (1993).

[6] W. Bao, S. Jin and P. A. Markowich, J. Comput. Phys. **175** (2002) 487.

[7] W. Bao and L. Yang, J. Comput. Phys. **225** (2007) 1863.

[8] G. M. Murlu and H. A. Erbay, Comput. Math. Appl. **45** (2003) 503.

[9] H. Borluk, G. M. Murlu, and H. A. Erbay, Math. Comput. Simulat. **74** (2007) 113.

[10] D. Bai and J. Wang, Commun. Nonlinear Sci. Numer. Simulat. **17** (2012) 1201.

[11] H. Wang, J. Comput. Phys. **205** (2007) 88.

[12] P. A. Markowich, P. Pietra, and C. Pohl, Numer. Math. **81** (1999) 595.

[13] L. M. Zhang and D. M. Bai, Inter. J. Comput. Math. **88** (2011) 1714.

[14] L. M. Zhang and F. Liao, Numer. Methods Partial Differential Equations **32** (2016) 1667.

[15] L. Y. Huang, Y. D. Jiao, and D. M. Liang, Chin. Phys. B. **22** (2013) 1.

[16] F. Liao and L. M. Zhang, Int. J. Comput. Math. **22** (2017) 1.

[17] L. M. Zhang, D. M. Bai, and S. S. Wang, J. Comput. Appl. Math. **235** (2011) 4899.

[18] S. Saha Ray, Z. Naturforsch. A **70** (2014) 659.

[19] S. Saha Ray and S. Sahoo, Math. Meth. Appl. Sci. **38** (2015) 2840.

[20] C. Celik and M. Duman, J. Comput. Phys. **231** (2012) 1743.